Solid-State Electronics Vol. 28, No. 5, pp. 427–433, 1985
Printed in Great Britain

0038–1101/85 $3.00 + .00
Pergamon Press Ltd.

THE ANNEALING OF 1 MeV IMPLANTATIONS OF BORON IN SILICON

S. OOSTERHOFF and J. MIDDELHOEK
Twente University of Technology, P.O. Box 217, 7500 AE Enschede, The Netherlands

(*Received* 19 *December* 1983; *in revised form* 5 *June* 1984)

Abstract—Buried layers of boron in silicon have been made by 1 MeV implantations up to a dose of 10^{13} cm^{-2}. The annealing of the implantation damage has been studied with Van der Pauw and Hall measurements. It is concluded that lattice damage reduces the mobility only for annealing temperatures below 600°C. The average mobilities measured after annealing at temperatures above 600°C correspond accurately to the values calculated from the most recent literature data, based on scattering by the lattice and by the active impurities. Complete activation was obtained after 60 min annealing at 700°C.

INTRODUCTION

High-energy implantations have not yet found much application in IC fabrication. In the late 1960s and early 1970s several papers [1–5] were published on high-energy implantation, mainly dealing with ranges and profiles. At present safe and reliable high-voltage implanters are available, and a growing interest is expected[6] for high-energy implantations.

Before our research on the applications of the high-energy implantations was started, a careful investigation of the thermal annealing of low-dose high-energy boron implantations was performed.

EXPERIMENTAL

Implantations

Implantations were carried out with a 500 kV HVEE implanter. We obtained 1 MeV ions by using doubly charged boron ions. There is no difference in range and straggling between doubly charged and singly charged ions having the same energy.

This is known from Blamires and Smith[7] and was checked by us by comparing a 250 kV B^{2+} implantation with a 500 kV B^{+} implantation, having the same dose (Fig. 1). These profiles were determined by a CV measurement as described in Ref. [8], using an MSI profiler. A disadvantage of using doubly charged ions is that the yield of doubly charged compared to singly charged boron ions is a little over 1%.

Process

The anneal process is studied by the repeated measurement of the sheet resistance on a Van der Pauw structure[8]. The outline of the structure is shown in Ref. [10]. Processing was started with thermally growing a 2 μm thick silicon dioxide layer on a selected *n*-type wafer of 7 Ω cm (Fig. 2(a)). This thickness of oxide was required for masking because of the great penetration depth of 1 MeV boron ions in silicon.

Next, diffusion areas were etched, and heavily *in situ* boron-doped polysilicon was deposited applying LPCVD at quasi-high flow [11] (Fig. 2(b)).

Doped polysilicon was applied for two reasons. First to act as a diffusion source to make contact with the deep implanted layer, and secondly to supply contact pads. Polysilicon interconnections were used because they can withstand temperatures up to 1400°C. Next the implantation area was etched to bare silicon and 1 MeV boron ions were implanted with a total dose of 10^{13} cm^{-2}. In order to avoid channeling, the wafers were tilted 7° (Fig. 2(c)).

After implantation, the interconnections were defined by etching the polysilicon. Processing was finished by depositing a 3000 Å thick silicon dioxide layer by means of CVD at 350°C for 7 min (Fig. 2(d)). Thus a first short anneal already took place

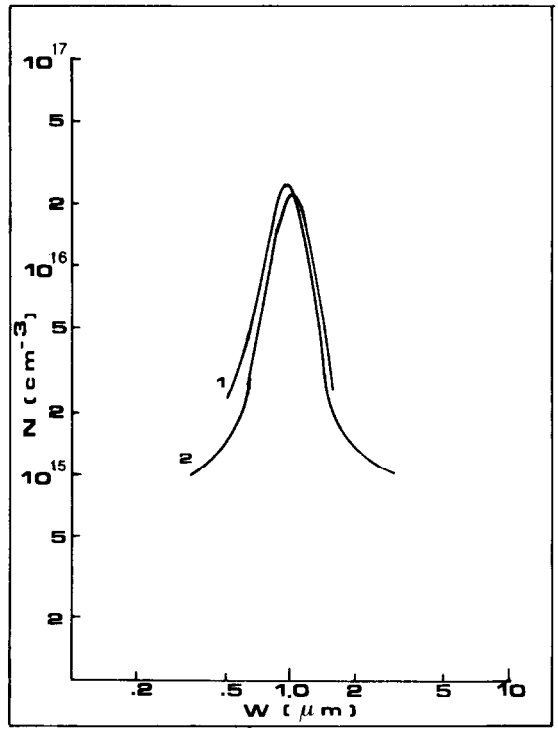

Fig. 1. Comparison of a 250 kV B^{2+} implant: (1) with a 500 kV B^{+} implant: (2) dose 10^{12} cm^{-2}.

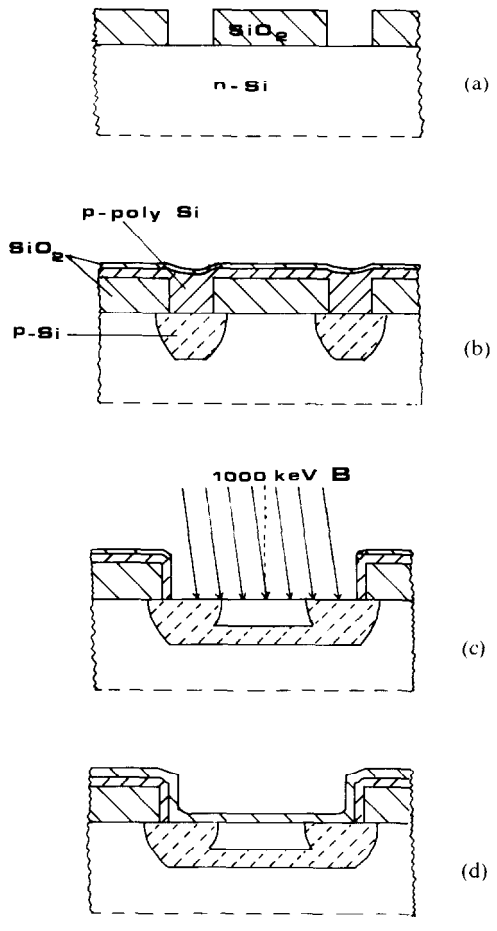

Fig. 2. Short process description, see explanation in the text.

during this step. In this protective oxide layer, contact windows were etched.

Annealing

The anneal experiments were carried out in a standard oxidation furnace in an oxygen ambient. Each wafer was annealed at one temperature in the range between 400 and 900°C. The time of each anneal step ranged from 5 min for the first few steps, to 30 min for the last step, to a total anneal time of 240 mins. Sheet resistances of 80 predetermined structures per wafer were measured after every anneal step.

Hall measurements

The Hall measurements were performed after finishing the anneal treatments. Three chips per wafer, consisting of four Van der Pauw structures each, were selected for Hall measurements. The chips were mounted and bonded on thick film substrates. Applied magnetic fields ranging from 0 to 4.5 kgauss and sample currents ranging from 100 to 300 A gave rise to Hall voltages up to 30 mV.

RESULTS AND DISCUSSION

Sheet conductance

Figure 3 shows the sheet conductance vs the anneal time. The sheet conductance is plotted because this quantity is directly proportional to the number of carriers and to the mobility. It is very remarkable that at each temperature a saturation value is reached within a short time. It seems that at a certain

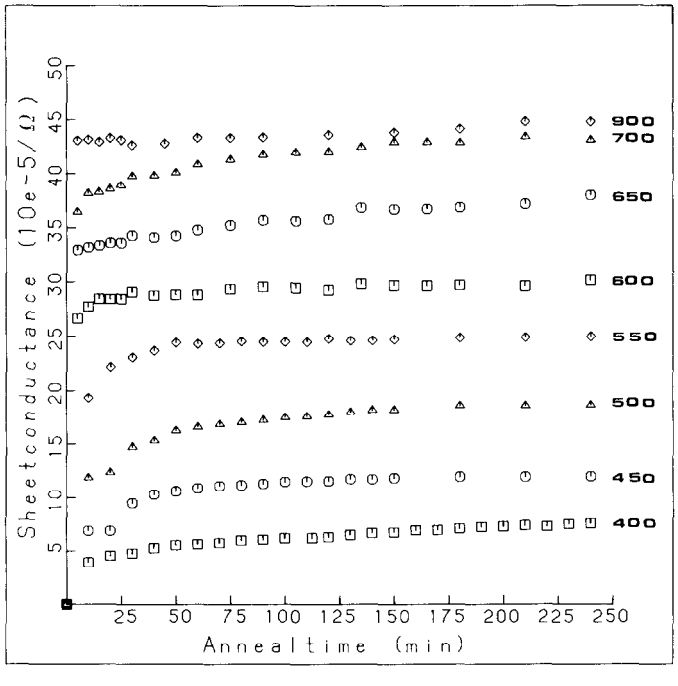

Fig. 3. Sheet conductance of a 10^{13} cm $^{-2}$ boron implant vs anneal time for different anneal temperatures.

temperature only a limited fraction of the carriers can be activated. This fraction increases proportionally with temperature in the range from 400 to 700°C. At temperatures of 700°C and above, however, complete activation is reached. In the case of 700°C it still takes approximately 1 h to reach this saturation value. The data for the experiments at 750, 800, and 850°C coincide with the 900°C data and are not shown here. The resistance values resulting from 4 h anneal at different temperatures, agree well with those from low-energy implanted resistors, as determined by Rosendal [12].

At the higher temperatures, complete activation is reached within the shortest anneal period (5 min). It was not possible to use shorter anneal times, because loading of the furnace and heating up and cooling down times prevented reproducible anneal times shorter than 5 min.

From Fig. 3 we see that the sheet conductance increases gradually with temperature, and as we will see later, this is mainly caused by a gradual increase with temperature of the number of carriers. Although several approaches were tried, we could not find a model that explained the experimental data.

In Fig. 4 the result of a separate series of experiments is shown. One wafer received successively a 30 min anneal at temperatures increasing from 450 to 1000°C. This experiment was carried out to test whether a multistep anneal gives better results than a single step anneal, at these low doses. The result was negative. The same minimum sheet resistance was reached as in the single step experiments shown in Fig. 3. The curve of Fig. 4 coincides with a cross section of Fig. 3.

Hall measurements

Carrier mobility and number of carriers were calculated from Hall sheet coefficients [13]. In these calculations the Hall factor r is assumed to be 0.8. This value is suggested for moderately doped p-type material by the majority of experimental results [14] and by recent calculations [15,16]. Also in these investigations 0.8 appeared to be an appropriate value.

The number of carriers is plotted vs the anneal temperature in Fig. 5. Experimental errors in this figure are smaller than the size of the square indicating the data point. The number of carriers increases gradually with anneal temperature up to 700°C, where it reaches a saturation value. This value agrees excellently with the implanted dose (10^{13} cm^{-2}). The experimental accuracy allows us to conclude that

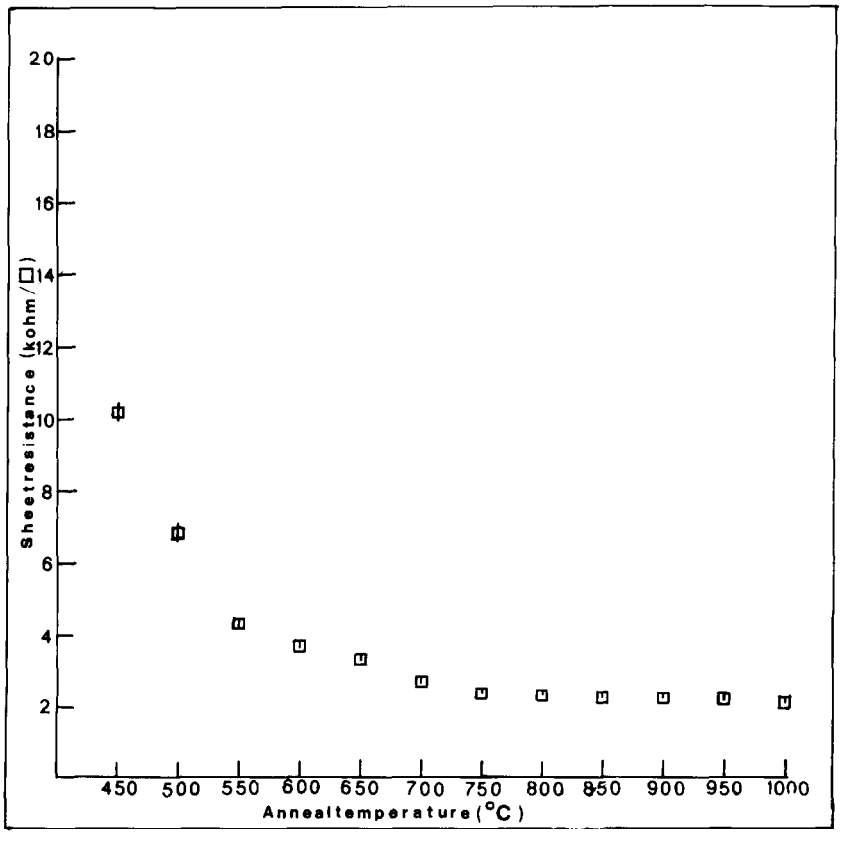

Fig. 4. Sheet resistance of a 10^{13} cm^{-2} boron implant vs anneal temperature at 30 min subsequent anneal time.

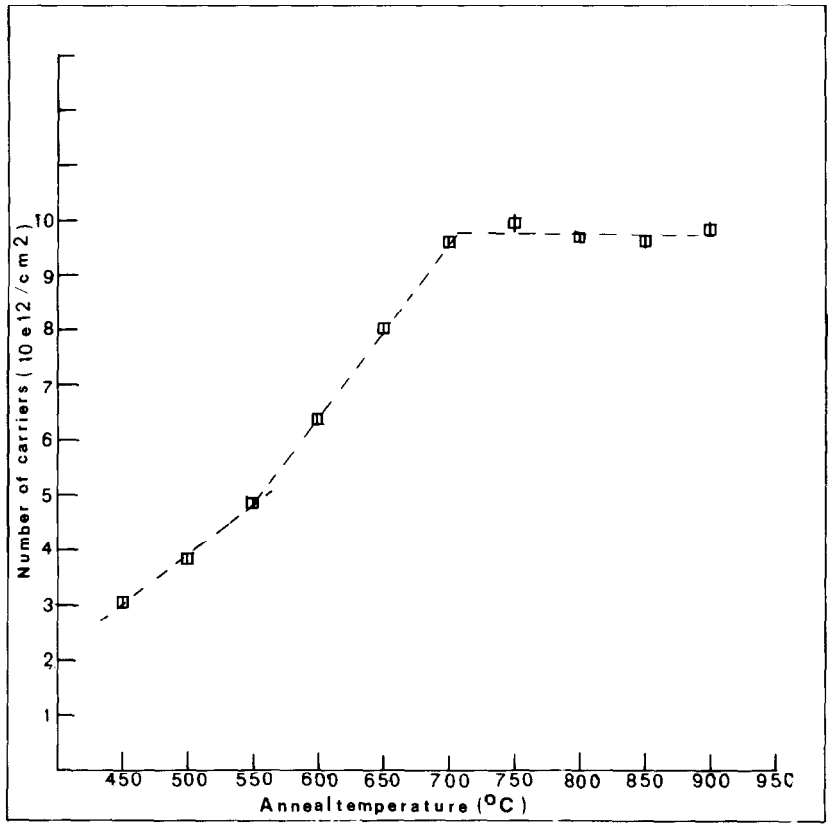

Fig. 5. Number of carriers vs anneal temperature for a 10^{13} cm^{-2} boron implant.

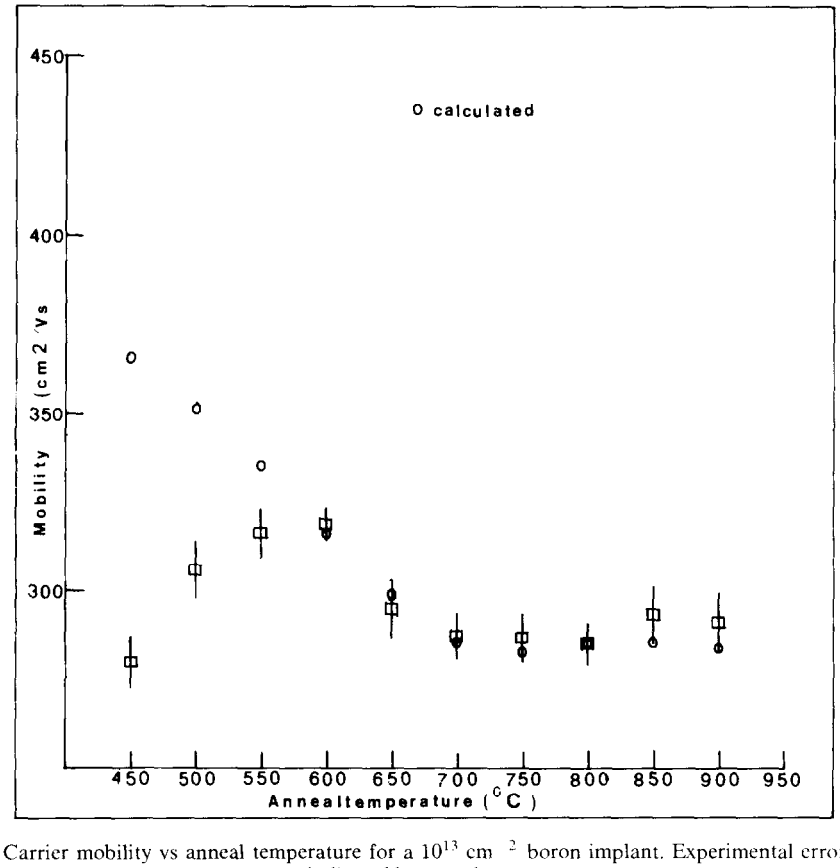

Fig. 6. Carrier mobility vs anneal temperature for a 10^{13} cm^{-2} boron implant. Experimental errors are indicated by error bars.

there are three different regions:

(I) anneal temperatures from 450 to 550°C,

(II) anneal temperatures from 500 to 700°C,

(III) anneal temperatures from 700 to 900°C.

This same distinction can be made in Fig. 6, where the carrier mobility is plotted vs the anneal temperature. This graph has a peculiar form: the mobility increases to a maximum at an anneal temperature of 600°C, decreases again, and reaches a saturation value at 700°C.

Our explanation is as follows: in the first region the mobility increases with temperature because of the restoration of the lattice. At about 600°C the restoration process is completed. The decrease of the mobility in region II is not caused by the phenomenon known in the literature[17,18] as reverse anneal, but simply by scattering by increasing numbers of active impurities. The concentration of the boron atoms is of the order of 10^{17} cm^{-3} so the mobility is very sensitive to changes in the concentration of impurities (see the mobility vs impurity concentration graph, e.g. in Ref. [15]).

The difference in slope between the first and the second region in Fig. 5 suggests that the number of carriers is also determined by the damaged lattice, because the number of carriers seems to be enhanced by the defects.

In region III, above 700°C, there is no change in the mobility, because all impurities are activated.

We repeated the Hall measurements for an implantation dose of 5×10^{11} cm^{-2}, having its peak concentration in the region where changes in the number of impurities hardly influence the mobility. The number of carriers vs the anneal temperature of this experiment is plotted in Fig. 7. This graph has basically the same form as Fig. 5, but because of the low dose, there is greater experimental inaccuracy in the data.

From Fig. 5 we concluded that for a dose of 10^{13} cm^{-2} complete activation was reached above 700°C, because the number of carriers appeared to be equal to the implanted dose. At a dose of 5×10^{11} cm^{-2}, 10% will be compensated by the bulk doping. Complete activation would thus lead to a net number of 4.5×10^{11} cm^{2}. Figure 7 shows that this is not the case. The number of carriers is only 2.5×10^{11} cm^{-2}.

In Fig. 8 the experimental average mobilities in the layer are plotted as a function of the anneal temperature. These mobilities are compared with calculated average mobilities, using the expression from Thurber

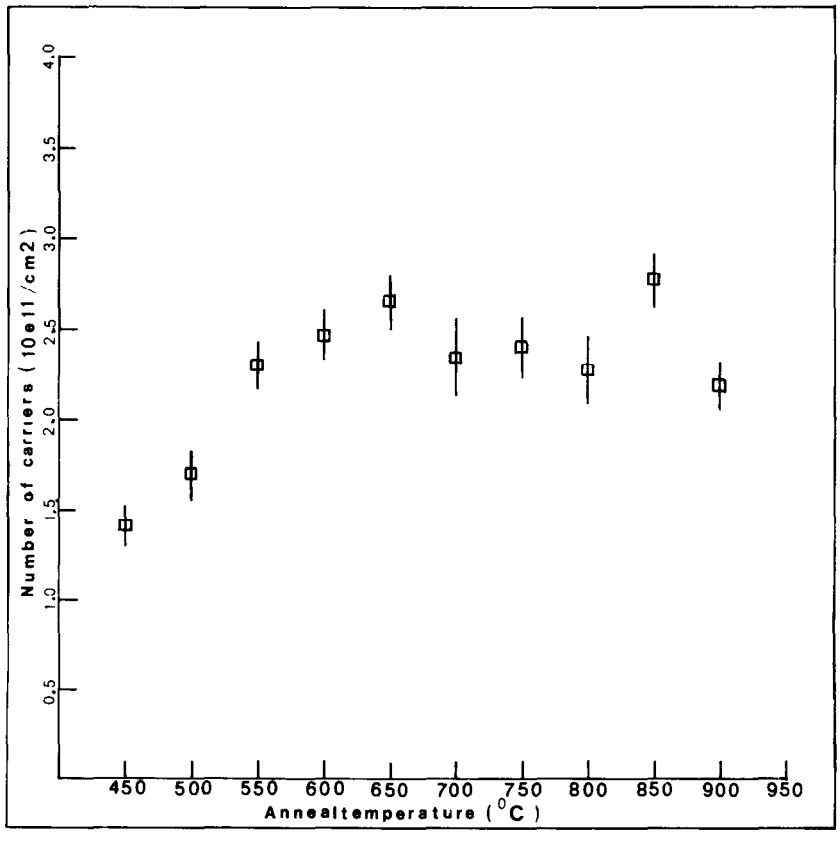

Fig. 7. Number of carriers vs anneal temperature for a 5×10^{11} cm^{-2} boron implant. Experimental errors are indicated by error bars.

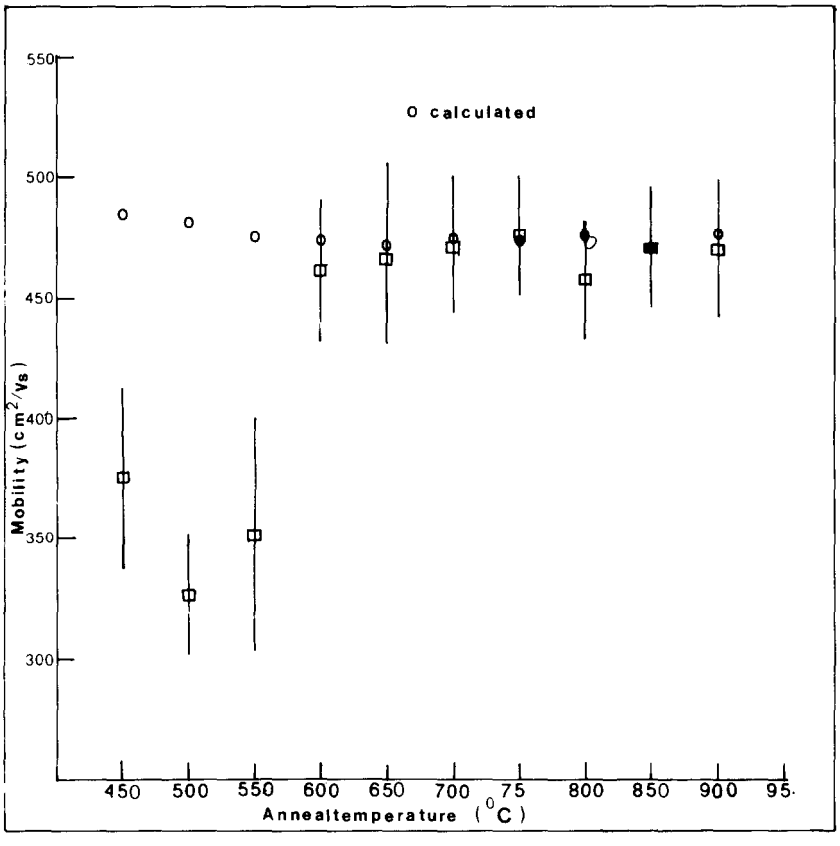

Fig. 8. Carrier mobility vs anneal temperature for a 5×10^{11} cm $^{-2}$ boron implant. Experimental errors are indicated by error bars.

et al.[15]. These calculations were performed using the experimentally determined numbers of carriers (see the Appendix).

These calculated mobilities are also shown in Fig. 8. In the first part of this graph (450–550°C) there is no agreement between experimentally determined and calculated values of the mobility. This can be explained by the fact that lattice damage is dominating the mobility. For temperatures above 600°C, there is a good agreement between experimentally determined and calculated mobilities. This leads to the conclusion, that the experimentally determined numbers of carriers, as plotted in Fig. 7, are real. It appears therefore, that complete activation is not reached at this low-dose implantation, even after annealing the sample for 4 h at 900°C.

A possible explanation for this incomplete activation might be that a fixed number of implanted boron ions reacts with contaminants (such as carbon, iron, oxygen, or lattice defects) already present in the starting material. This would give rise to a fixed loss in the number of carriers. The loss must be a small fixed number, and not a fraction of the total implanted dose, because for a dose of 10^{13} cm^{-2} complete activation is reached within experimental accuracy.

In Fig. 6 mobilities are also shown, calculated from the corresponding numbers of carriers from Fig. 5. These calculations strengthen the explanation we gave before. In the lower temperature region (450–550°C) lattice damage dominates the mobility. In the other two regions, there is an excellent agreement between calculated and experimentally determined mobilities.

CONCLUSIONS

It is difficult to explain the anneal behaviour of deep implanted layers, because for every anneal temperature, a different saturation value is found for the sheet resistance.

A multistep anneal gives the same value of the sheet resistance as a single step anneal at the highest temperature of the multistep anneal at low dose.

Complete activation of the implanted impurity needs annealing for at least 60 min at 700°C. The restoration of the lattice seems already to be complete at 600°C.

For low-dose implantations it appears that approximately 2.5×10^{11} cm^{-2} does not become active. Below 600°C the mobility is dominated by lattice damage. The average mobility of an activated buried implanted layer can be calculated using the formulae of Thurber. A multistep anneal gives the same results for the sheet resistance at low dose.

Acknowledgements—These investigations in the program of the Foundation for Fundamental Research on Matter (FOM) have been supported by the Foundation for Technical Research (STW), future Technical Science Branch/Division of the Netherlands Organization for the Advancement of Pure Research (ZWO). Furthermore, the authors would like to thank J. Holleman, A. Kooy, and A. Aarnink for giving valuable help during the processing of the samples and H. ter Riet for fabrication of the thick-film substrates.

REFERENCES

1. S. Roosild, R. Dolan and B. Buchanan, *J. Electrochem. Soc.* **115**, 307 (1968).
2. A. Kostka and S. Kalbitzer, *Radiat. Eff.* **19**, 77 (1973).
3. D. E. Davies, *Solid-St. Electron.* **13**, 229 (1970).
4. E. W. Maby, Ph.D. Thesis, Massachusetts Institute of Technology, Cambridge (1979).
5. W. K. Hofker, *Philips Res. Rep.* Suppl. No. 8 (1975).
6. J. F. Ziegler, private communication.
7. N. G. Blamires and B. J. Smith, *J. Phys. D.* **10**, 799 (1977).
8. D. L. Rehrig and C. W. Pearce, *Semicond. Int.* **3**, 151 (1980).
9. L. J. v. d. Pauw, *Philips Res. Rep.* **13**, 1 (1958).
10. S. Oosterhoff and J. Middelhoek, *Proc. 4th Int. Conf. on Ion Impl.: Equipment and Techniques* (Edited by H. Glawischnig and H. Ryssel), p. 438. Springer, Berlin (1983).
11. J. Holleman and J. Middelhoek, *Thin Solid Films* **114**, 295 (1984).
12. K. Rosendal, *Radiat. Eff.* **7**, 95 (1971).
13. G. Carter and W. Grant, *Ion Implantation of Semiconductors*, p. 180. Edward Arnold, London (1976).
14. D. K. Schroder, T. T. Braggins and H. M. Hobgood, *J. Appl. Phys.* **49**, 5256 (1978).
15. W. R. Thruber, R. L. Mattis, Y. M. Liu and J. J. Filliben, *J. Electrochem. Soc.* **127**, 2291 (1980).
16. G. Massetti, M. Severi and S. Solmi, *IEEE Trans. Electron Devices* **30**, 764 (1983).
17. T. E. Seidel and A. U. MacRae, *Int. Conf. on Ion Impl. in Semicond.* (Edited by L. T. Chadderton and F. H. Eisen), Vol. 149. Gordon & Breach, London (1971).
18. H. Ryssel and I. Ruge, *Ion Implantation*, p. 57. B. G. Teubner, Stuttgart (1978).
19. B. Smith, *Ion Implantation Range Data for Silicon and Germanium Device Technologies*. Learned Information, Oxford (1977).

APPENDIX

Calculation of the average mobility of an implanted buried layer

In this calculation, we use the curve-fits from Thurber *et al.*[15] for the hole mobility at two different temperatures as a function of the hole density

$$\mu = A \exp\left(-\frac{p_c}{p}\right) + \frac{\mu_{\max}}{1+\left(\frac{p}{p_{\text{ref}}}\right)^{\alpha}}. \tag{A1}$$

With a linear extrapolation of the data from Thurber, we found for $T = 19°C$

$$A = 45.5 \text{ cm}^2 \text{ V}^{-1} \text{ s}^{-1}, \quad \mu_{\max} = 501.7 \text{ cm}^2 \text{ V}^{-1} \text{ s}^{-1},$$

$$p_c = 8.77 \times 10^{16} \text{ cm}^{-3}, \quad p_{\text{ref}} = 2 \times 10^{17} \text{ cm}^{-3},$$

$$\alpha = 0.717.$$

We assume the hole density $p = p(x)$ to have the same shape as the impurity profile.

This profile is approximated by a Gaussian curve

$$p(x) = p_{\max} \exp\left\{-\frac{1}{2}\left(\frac{x - R_p}{\Delta R_p}\right)^2\right\}, \tag{A2}$$

with $p_{\max}$ being the peak concentration, defined by

$$p_{\max} = \frac{n}{\sqrt{(2\pi)}\,\Delta R_p}. \tag{A3}$$

Values of projected range and straggling are taken from Smith [19],

$$R_p = 1.647\,\mu\text{m},$$

$$\Delta R_p = 0.124\,\mu\text{m}.$$

And n is the number of carriers extracted from Figs. 5 and 7.

The average mobility of a buried implanted layer is calculated by integrating the hole mobility over the impurity profile

$$\bar{\mu} = \frac{\int \mu_H p(x)\,\mathrm{d}x}{\int p(x)\,\mathrm{d}x}. \tag{A4}$$

The denominator of eqn (A4) is by definition the number of carriers n. As integration boundaries were chosen: $3.5\,\Delta R_p$ and $-3.5\,\Delta R_p$, covering 99.9% of the number of carriers.

Insertion of eqns (A1) and (A2) into eqn (A4) and substituting $(x - R_p)/\Delta R_p$ by y leads to

$$\bar{\mu}_n = 2A p_{\max} \int_0^{3.5} \exp\left(-\frac{y^2}{2}\right) \exp\left\{\frac{-p_c}{p_{\max}}\, e^{y^2/2}\right\} \mathrm{d}y$$

$$+ 2 p_{\max} \mu_{\max} \int_0^{3.5} \exp\left(-\frac{y^2}{2}\right)$$

$$\times \left[1 + \left(\frac{p_{\max} \exp\left(-\frac{y^2}{2}\right)}{p_{\text{ref}}}\right)^{\alpha}\right]^{-1} \mathrm{d}y. \tag{A5}$$

This equation was solved numerically.